

Interplay of Coulomb attraction and spatial confinement in the optical susceptibility of quantum wires

S. Glutsch and F. Bechstedt

Institut für Festkörpertheorie und Theoretische Optik, Friedrich-Schiller-Universität, Max-Wien-Platz 1, O-6900 Jena, Germany

(Received 28 September 1992)

Arrays of quantum-well wires are described within the envelope-function formalism. Starting from a generalization of the well-known Elliott formula, the optical susceptibility can be related to solutions of an effective two-particle Schrödinger equation including both Coulomb interaction and the modulation of the band edges due to the wire array structure. For frequencies near the absorption edge the imaginary part of the susceptibility is numerically calculated. The influence of thickness fluctuations on the spectra is discussed, too. Numerical calculations are compared with luminescence spectra of arrays fabricated by laser-induced thermal interdiffusion.

The spectroscopy of optical interband transitions across the band gap is a powerful method for studying the electronic structure, the mutual interaction of excited electrons (*e*) and holes (*h*), and the coupling of these carriers with other elementary excitations in semiconductors and semiconductor microstructures. Very interesting systems in this respect are quantum-well wires and quantum-well-wire (QWW) arrays. In such quasi-one-dimensional (1D) structures made by epitaxial growth of III-V semiconductor layers and nanostructuring techniques, quantum confinement in two dimensions is realized.

Some effects attributed to quantum confinement and anisotropy of the wire systems have already been observed in photoluminescence and photoluminescence excitation spectra.¹⁻⁸ Most of the QWW structures studied by optical methods have been prepared by starting from GaAs-Al_xGa_{1-x}As layered systems and employing modern lithographic techniques;⁹ however, they are commonly combined with etching techniques, which produce rough surfaces of the wire structures resulting in peaks that are broader than those of the corresponding 2D system.⁶ Very recently, more perfect QWW structures have been manufactured via Al-Ga interdiffusion due to local heating by means of a focused laser beam.⁸ The quality of these samples is characterized by excitonic luminescence lines that are smaller, as in the 2D case.

In the optical-absorption and luminescence spectra, excitonic effects play an important role, particularly in the low-dimensional QWW systems. However, in contrast to the exact 3D or 2D case, to our knowledge no unified picture of the Coulomb effects in these spectra has been presented. Binding energies of the excitons have been calculated^{10,11} and Sommerfeld factors of exact 1D systems with modified Coulomb potentials have been studied.¹² The optical function of a parabolic wire is calculated in the limit of vanishing coupling of wire subbands.¹³

In the present paper, we develop a complete theory for optical-absorption and luminescence spectra of a quantum-well-wire array, including the Coulomb attraction of an electron and hole excited by a photon for fre-

quencies near the absorption edge. The two-particle equation is solved numerically for energies and confinements characterizing the experimental situation. Hence, the presented theory is valid for all wire thicknesses and wire arrangements. The theoretical results are compared with experimental data.

The optical properties of the system are characterized by the space-dependent linear optical susceptibility. For frequencies near the absorption edge, it can be obtained using a density-matrix formalism such as

$$\chi(\mathbf{x}, \mathbf{x}'; \omega) = \frac{2}{\epsilon_0} |\mu|^2 \sum_{\alpha} \frac{\Phi_{\alpha}(\mathbf{x}, \mathbf{x}) \Phi_{\alpha}^*(\mathbf{x}', \mathbf{x}')}{E_{\alpha} - \hbar(\omega + i\Gamma)}. \quad (1)$$

It is directly related to electron-hole-pair wave functions $\Phi_{\alpha}(\mathbf{x}_e, \mathbf{x}_h)$ and energies E_{α} , with α as the complete set of quantum numbers for the two-particle problem. ϵ_0 denotes the vacuum dielectric constant and Γ indicates the damping of the electron-hole pairs. Obviously, Eq. (1) represents a generalization of the well-known Elliott formula.¹⁴ The nonlocal linear optical susceptibility (1) is not directly observed in absorption and luminescence measurements but in an effective measurement that can be obtained from (1) by a twofold integration running over \mathbf{x}, \mathbf{x}' . Physically such a procedure means an averaging over the incoming and outgoing fields.

In the framework of the effective-mass approximation and masses m_e (m_h) of electrons (holes), the two-particle wave functions obey a Schrödinger equation of the form

$$\left[-\frac{\hbar^2}{2} \nabla_{\mathbf{x}_e} \cdot \frac{1}{m_e} \cdot \nabla_{\mathbf{x}_e} + V_e(\mathbf{x}_e) - \frac{\hbar^2}{2} \nabla_{\mathbf{x}_h} \cdot \frac{1}{m_h} \cdot \nabla_{\mathbf{x}_h} + V_h(\mathbf{x}_h) - \frac{e^2}{4\pi\epsilon_0 |\mathbf{x}_e - \mathbf{x}_h|} \right] \Phi_{\alpha}(\mathbf{x}_e, \mathbf{x}_h) = E_{\alpha} \Phi_{\alpha}(\mathbf{x}_e, \mathbf{x}_h), \quad (2)$$

where electrons and holes interact by a Coulomb potential screened by a relative static dielectric constant ϵ of the underlying semiconductor material forming the wires. The complications in the screening due to the realistic spatial structure of the system¹⁵ are avoided, assuming

that the dielectric constants of wire and barrier materials are not so very different as in the case of GaAs and $\text{Al}_x\text{Ga}_{1-x}\text{As}$.

Equation (2) in general represents a six-dimensional Schrödinger equation that holds for arbitrary confinement in the systems within the envelope-function approximation. We suppose that the quantization of the underlying quantum-well (QW) structure in the z direction is much stronger than the wire quantization in the y direction, and that the confinement potentials $V_i(\mathbf{x}_i)$ ($i=e,h$) can be separated with respect to the corresponding coordinates. In this limit the quantization energies due to the underlying well are large enough so that the corresponding peaks in the optical spectrum are well separated. We can focus our attention on frequencies around the first heavy-hole exciton peak. Practically only the first well subband is taken into account. The z dependences in the susceptibility and in the two-particle equation can be averaged with respect to the corresponding electron and hole wave functions. Equation (1) reduced now to an expression depending only on the motion in the xy plane:

$$\chi(\mathbf{r}, \mathbf{r}', \omega) = \frac{2}{\epsilon_0} |\mu|^2 N_z \sum_{\beta} \frac{\Phi_{\beta}(\mathbf{r}, \mathbf{r}) \Phi_{\beta}^*(\mathbf{r}', \mathbf{r}')}{E_{\beta} - \hbar(\omega + i\Gamma)}, \quad (3)$$

$$N_z = \left| \int_{-\infty}^{\infty} dz \varphi_{e1}(z) \varphi_{h1}(z) \right|^2, \quad \mathbf{r} = (x, y).$$

$\varphi_{e1}, \varphi_{h1}$ are the first QW eigenfunctions of the electron and hole, respectively. They are calculated for a finite square-well potential. The functions Φ_{β} now obey a four-dimensional Schrödinger equation:

$$\left[-\frac{\hbar^2}{2m_e} \Delta_{\mathbf{r}_e} + V_{ye}(y_e) - \frac{\hbar^2}{2m_h} \Delta_{\mathbf{r}_h} + V_{yh}(y_h) - V_{\text{Coul}}(|\mathbf{r}_e - \mathbf{r}_h|) \right] \Phi_{\beta}(\mathbf{r}_e, \mathbf{r}_h) = E_{\beta} \Phi_{\beta}(\mathbf{r}_e, \mathbf{r}_h). \quad (4)$$

$V_{ye}(y_e), V_{yh}(y_h)$ represent the wire confinement potentials. The averaged 2D Coulomb potential is given by

$$V_{\text{Coul}}(r) = \frac{e^2}{4\pi\epsilon_0\epsilon} \int_{-\infty}^{\infty} dz_e \int_{-\infty}^{\infty} dz_h \frac{|\varphi_{e1}(z_e)|^2 |\varphi_{h1}(z_h)|^2}{\sqrt{r^2 + (z_e - z_h)^2}}. \quad (5)$$

The well approximation in the first electron and hole subbands also enters the definition of the pair energies E_{α} via the 2D energy gaps. Equation (4) can be simplified further by separation of the center-of-mass motion in the x direction. The remaining partial differential equation cannot be solved analytically, except in the case of parabolic wire potentials and e - h symmetry. This model can explain some basic features of dielectric and optical properties of quantum-well wires.^{16,17} However, in this paper we will treat more realistic confinement situations by the numerical solution of Eq. (4).

The samples studied experimentally consist mostly of arrays of QW's. Large arrays exhibit a 1D translational symmetry with the lattice constant a ; more strictly, it holds that $V_{iy}(y_i + a) = V_{iy}(y_i)$ ($i=e,h$). Introducing the

center of mass and coordinates X, Y and relative coordinates x, y , and separating the center-of-mass motion in the x direction, the Bloch theorem can be applied for the dependence of the solutions of Eq. (4) on the Y coordinate. The resulting optical susceptibility is then given by

$$\chi(\omega) = \frac{2}{\epsilon_0} |\mu|^2 N_z \sum_n \frac{\frac{1}{\alpha} \left| \int_{-a/2}^{a/2} dY \varphi_n(Y, x=0, y=0) \right|^2}{E_n - \hbar(\omega + i\Gamma)}, \quad (6)$$

where the wave functions φ_n have to be determined by solving the eigenvalue problem:

$$\left[-\frac{\hbar^2}{2M} \frac{d^2}{dY^2} - \frac{\hbar^2}{2m} \Delta_{\mathbf{r}} + V_{ye}(y_e) V_{yh}(y_h) - V_{\text{Coul}}(r) \right] \times \varphi_n(Y, x, y) = E_n \varphi_n(Y, x, y), \quad (7)$$

with coordinates and masses $Y = m_e y_e + m_h y_h / M$, $\mathbf{r} = \mathbf{r}_e - \mathbf{r}_h$, $M = m_e + m_h$, and $m = m_e m_h / M$.

The remaining Schrödinger equation (7), depending on the three coordinates Y, x , and y , has been solved numerically by application of a Rayleigh-Ritz-Galerkin method.¹⁸ In further considerations all quantities are expressed in excitonic units of the bulk material, Rydberg energy E_B , and Bohr radius a_B , respectively. For GaAs it holds at about $E_B = 4$ meV, $a_B = 10$ nm. In these units, we choose $\Delta E_c = 12E_B, \Delta E_v = 8E_B$ for the band discontinuities between GaAs and $\text{Ga}_{0.65}\text{Al}_{0.35}\text{As}$.¹⁹ In a certain region, the interdiffusion is assumed to be complete, and rapidly decreasing beyond it. In the case of interdiffused wire systems, we assume the following form for the confinement potentials:

$$V_{ye/h}(y) = \pm \frac{1}{2} E_g^{(2)} \pm \Delta \tilde{E}_{c/v} [f(y) - 1],$$

$$f(y) = \frac{c_1(y) + c_2(y)}{1 + c_1(y)c_2(y)}, \quad (8)$$

$$c_{1/2}(y) = \begin{cases} 1 & \text{for } \frac{a}{2} \pm y < \lambda \\ \exp \left[-\frac{\left[\frac{a}{2} \pm y \right]^2}{2\mu^2} \right] & \text{for } \frac{a}{2} \pm y \geq \lambda, \end{cases}$$

$$c_{1/2}(y + a) = c_{1/2}(y),$$

with the parameters $\lambda = 7.0a_B, \mu = 0.5a_B$ which are able to describe the experimental conditions in Ref. 8. The characteristic length 2λ corresponds to the width of the interdiffusion profile along the laser scan line,⁸ i.e., the extent of the barrier between two wires, whereas $(a - 2\lambda)$ nearly represents the geometrical width of the wires. The wire distance a follows the distance between two written laser lines. $\Delta \tilde{E}_{c/v}$ represents the band discontinuities between the conduction (valence) band of the $\text{Ga}_{1-x}\text{Al}_x\text{As}$ material outside and the first electron (hole) subbands of the QW.

Figure 1 shows the imaginary part of the optical sus-

ceptibility for a well thickness $d = 0.25a_B$ and constant different wire distances a . The function $f(y) - 1$, governing the potential shape (8), is shown in the inset. A homogeneous linewidth $\Gamma = 0.05a_B/\hbar$ is introduced for a representation of the results. The zero point is given by the energy gap $E_g^{(2)}$ of the $\text{Ga}_{1-x}\text{Al}_x\text{As}$ barrier material outside. $(a - 2\lambda) = \infty$ (a) corresponds to the ordinary 2D situation. With decreasing wire widths (b)–(c), the influence of the center-of-mass quantization is visible and provokes a series of blueshifted peaks with lower oscillator strengths. Their distances are increasing with decreasing wire width. Since $(a - 2\lambda) \gg a_B$, the internal motion of the exciton is hardly influenced by the center-

of-mass motion, and vice versa. Therefore, for the total wave functions $\varphi_n(Y, x, y)$ from Eq. (7), it nearly holds that $\varphi_n(Y, x, y) = \Phi_N(Y)\varphi_{m_l}(x, y)$, where m represents the quantum number of the angular momentum. Since $\varphi_{m_l}(x, y) = O(r^m)$ for $r \rightarrow 0$, only the excitons with $l = 0$, i.e., the s excitons, contribute to the oscillator strength. The situation changes if $(a - 2\lambda)$ approaches a_B (d). The lowest peak in the spectrum is somewhat blueshifted due to the stronger quantization of the center-of-mass motion in the y direction. In addition, a fine structure of the lines split by the quantization of the center-of-mass motion appears. We are now faced with three effects. (i) The internal motion is essentially influenced by the wire

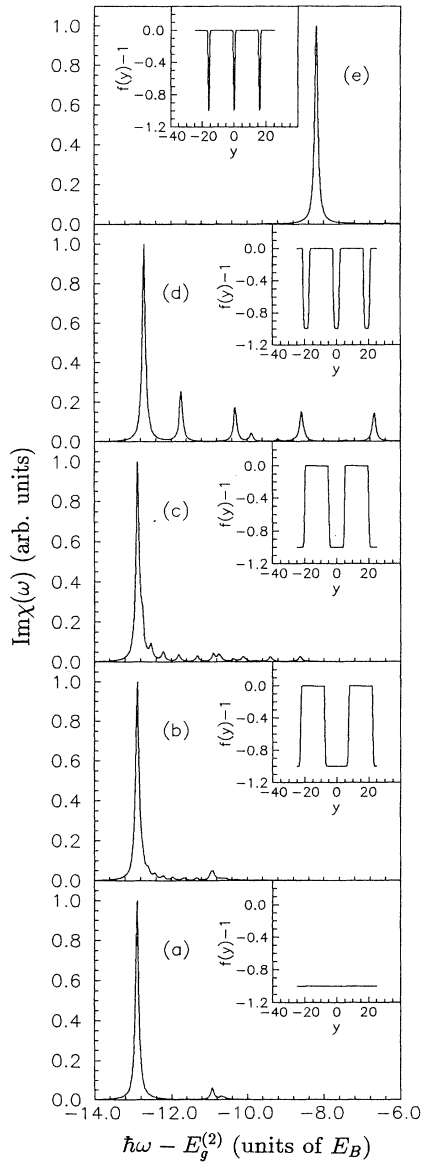


FIG. 1. The imaginary part of the optical susceptibility $\text{Im}\chi$ vs energy $\hbar\omega - E_g^{(2)}$ for different wire widths $a = \infty$ (a), 30 (b), 25 (c), 19 (d), and 17 (e). Inset: function $f(y) - 1$ vs y (in units of a_B).

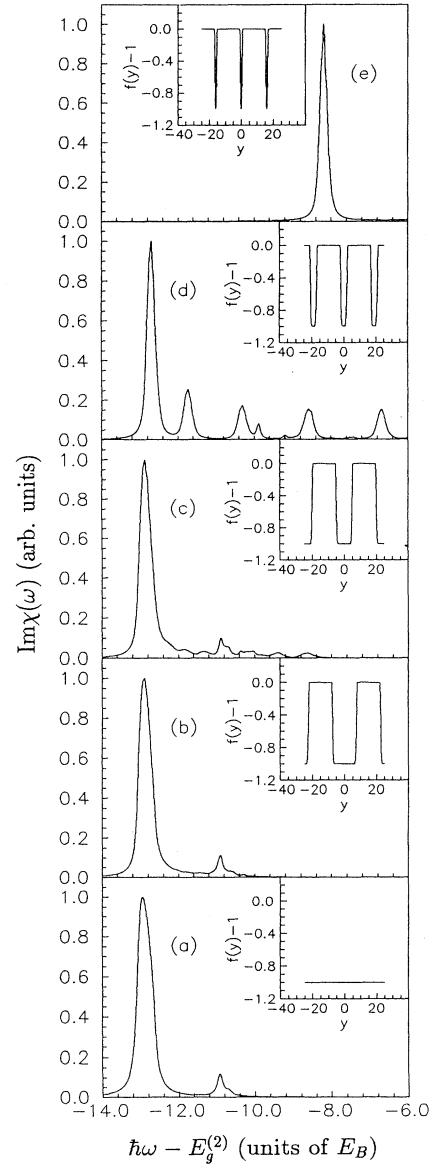


FIG. 2. The imaginary part of the optical susceptibility $\text{Im}\chi$ vs energy $\hbar\omega - E_g^{(2)}$. The well fluctuations are modeled by a Gaussian distribution of the well thickness d . The same parameters as in Fig. 1 are applied. Inset: function $f(y) - 1$ vs y (in units of a_B).

potentials. Especially the larger excitons are shifted toward higher energies, since the overlap integrals of their wave functions with the wire potentials are larger. (ii) The angular momentum of the internal motion is no longer conserved, therefore an intermixing of s, p, d, \dots excitons occurs. The break of the Coulomb degeneracy leads to additional peaks, since the wave functions now do not vanish for $r=0$. (iii) The center-of-mass motion itself is affected by the internal motion, but this influence is very small. This explains the fact that the principal features of the wire confinement can at least qualitatively be explained by neglecting the coupling between the center-of-mass and the internal motion.¹⁷ If the wire width is further reduced [Fig. 1(e)], only the $1s$ excitons remain in the wire, whereas the larger ones with higher quantum numbers are displaced energetically outside the wire. They lose their 1D character. For $a \rightarrow 2\lambda$ (not shown here), either the limiting case of a 2D semiconductor with larger E_g^{2D} , or the 3D case with the band gap $E_g^{(2)}$, is reached if the interdiffusion is complete. The detailed interpretation of the resulting spectra is complicated because the fine structure of the lifted Coulomb degeneracy in the internal exciton motion belonging to a particular peak N related to quantization of the center-of-mass motion occurs at positions shifted to higher energies. For typical quantization energies of the center-of-mass motion smaller than the 2D binding energy, it is observed close to peaks with quantum numbers larger than N .

This behavior is different from that of a narrow QW. Since in the QW case the 2D binding energy is limited by an amount of about $4E_B$, it is possible to carry out a transition from the "center-of-mass" quantization, where the total wave function Φ is nearly given by $\Phi(\mathbf{x}_e, \mathbf{x}_h) = e^{iK_x X + iK_y Y} \Phi_{cm}(Z) \varphi_{rel}(\mathbf{x})$, to the "size" quantization where $\Phi(\mathbf{x}_e, \mathbf{x}_h) = e^{iK_x X + iK_y Y} \varphi_e(z_e) \varphi_h(z_h) \varphi_{rel}(\mathbf{r})$. The latter case is impossible in the QWW with the y direction, because the 1D binding energy is not limited, and even for small wire widths the different wire subbands are never decoupled in the Coulomb potential. Therefore a solution of Eq. (7) in real space is better suited than an expansion of the Coulomb potential in terms of single-particle states of the wire potential. In order to compare with the experimental situation of Ref. 8, one has to take into account the fluctuation of the well thickness. As discussed above, the lines occurring in the spectrum (Fig. 1) cannot be related simply to quantum numbers of the center-of-mass and internal motions. Thus the introduction of phenomenological linewidths is not manageable. We will treat the rather complicated prob-

lem of a quantum-mechanical system in a stochastic potential by the following simple considerations: In the QW, the fluctuations will essentially affect the internal motion, whereas the wave function of the center-of-mass motion averages over the whole surface. If the well additionally is laterally structured and the wire barriers are nearly perfect, the influence of the well fluctuations tends to zero for vanishing wire width a . Therefore we average different spectra with a Gaussian distribution of the well thickness entering the 2D Coulomb potential (5) with a variance depending on the wire width. In Fig. 2, the influence of the well fluctuations on the optical spectra is shown. We have chosen $d_0 = 0.25a_B$, $\sigma_0 = 0.1a_B$, and $a_0 = 50a_B$; the other parameters are the same as in Fig. 1. As expected, the maxima of peaks for the $2s, 3s$, etc. excitons are now higher than in the case of an ideal QW (Fig. 1). This leads to a more pronounced fine structure when the wire width is on the order of few Bohr radii. As in the experiment, the inhomogeneous linewidths vary and reveal the origin of the corresponding peaks: the most broadened lines arise from $1s$ excitons with different center-of-mass eigenstates, whereas the smaller ones can be related to the $2s$ and higher excitonic states. A detailed comparison of the resulting spectrum with the experimental findings is complicated. Nevertheless, the most important features are observed in both types of spectra. They are (i) the appearance of nearly equidistant main peaks belonging to different states of the center-of-mass motion; and (ii) a fine structure, i.e., a series of small peaks at higher energies, due to the lifting of the Coulomb degeneracy in the wire potential. In the measured luminescence spectra, additional peaks and a certain background, both related to the real structure of the wire system, occur.

In the present paper, we have shown that the solution of the two-particle Schrödinger equation in real space is an efficient method for calculating the optical spectra of quantum wires with arbitrary wire potentials. The case of an array allows one to carry out the transition to the 2D case within the limit of infinitely large wire widths. Contrary to the quasi-2D case, 1D pure "size" quantization is impossible. For very small wire widths the excitons do not adopt quasi-1D character but leave the wire. The inhomogeneous broadening due to the well roughness leads to a stronger emphasis on the higher excitonic states compared to the ground state.

The authors are greatly indebted to G. Abstreiter, K. Brunner, J. Christen, D. Heitmann, H. Lage, and R. Zimmermann for helpful discussions.

¹Y. Hirayama, S. Tarucha, Y. Suzuki, and H. Okamoto, Phys. Rev. B **37**, 2774 (1988).

²D. Gershoni, H. Temkin, G. J. Dolan, J. Dunsmuir, S. N. G. Chu, and M. B. Panish, Appl. Phys. Lett. **53**, 995 (1988).

³M. Tsuchiya, J. M. Gaines, R. H. Yan, R. J. Simes, P. O. Holtz, L. A. Coldren, and P. M. Petroff, Phys. Rev. Lett. **62**, 466 (1989).

⁴M. Kohl, D. Heitmann, P. Grambow, and K. Ploog, Phys.

Rev. Lett. **63**, 2124 (1989).

⁵M. Tanaka, J. Motohisa, and H. Sakaki, Surf. Sci. **228**, 408 (1990).

⁶H. Lage, D. Heitmann, R. Cingolani, P. Grambow, and K. Ploog, Phys. Rev. B **44**, 6550 (1991).

⁷R. Cingolani, H. Lage, L. Tapfer, H. Kalt, D. Heitmann, and K. Ploog, Phys. Rev. Lett. **67**, 891 (1991).

⁸K. Brunner, G. Abstreiter, M. Walter, G. Böhm, and G.

- Tränkle, *Surf. Sci.* **267**, 218 (1992).
- ⁹K. Kash, *J. Lumin.* **46**, 69 (1990).
- ¹⁰T. Kodama and Y. Osaka, *Jpn. J. Appl. Phys.* **25**, 1875 (1986).
- ¹¹L. Banyai, I. Galbraith, C. Ell, and H. Haug, *Phys. Rev. B* **36**, 6099 (1987).
- ¹²T. Ogawa and T. Takagahara, *Phys. Rev. B* **43**, 14 325 (1991); **44**, 8138 (1991).
- ¹³S. Benner and H. Haug, *Europhys. Lett.* **16**, 579 (1991).
- ¹⁴R. J. Elliott, *Phys. Rev.* **108**, 1384 (1957).
- ¹⁵L. Wendler, F. Bechstedt, and M. Fiedler, *Phys. Status Solidi B* **159**, 143 (1990); *Superlatt. Microstruct.* **10**, 183 (1991).
- ¹⁶V. Halonen, in *Proceedings of the International Meeting on Optics of Excitons in Confined Systems, Giardini Naxos, 1991*, edited by A. D'Andrea, R. Del Sole, R. Girlanda, and A. Quattropani (Institute of Physics, Bristol, 1992), p. 313.
- ¹⁷S. Glutsch and F. Bechstedt, *Superlatt. Microstruct.* (to be published); *Proceedings of the 21st International Conference on the Physics of Semiconductors, Beijing, 1992* (World Scientific, Singapore, 1992).
- ¹⁸J. Stoer and R. Burlisch, *Introduction to Numerical Analysis* (Springer, New York, 1983).
- ¹⁹R. C. Miller, A. C. Gossard, D. A. Kleinman, and O. Munteanu, *Phys. Rev. B* **29**, 3740 (1984); R. C. Miller, D. A. Kleinman, and A. C. Gossard, *ibid.* **29**, 7085 (1984).